Lab report
K223 Nuclear γ-γ Angular Correlations

Chenhuan Wang and Harilal Bhattarai

August 30, 2020

In this experiment, we investigate nuclear properties of cobalt nuclei via angular correlation. With scintillation detectors, we measure number of coincidence in dependence on angle between two photons. There is strong anisotropy in coincidence rate present. The measured data are fitted with the theoretical prediction function and calculated the angular correlation coefficients: $A_{22} = 0.0849 \pm 0.0057$ and $A_{44} = -0.0002 \pm 0.0063$. Closer investigation reveals that measured values differ from prediction by 4σ. Other types of cascade are excluded almost 100%.

1 Introduction

In a cascade gamma decay of nuclei a non-isotropic angular distribution can be measured due to non-equilibrium spin state; however, in thermal equilibrium net orientation of all spin states is zero due to gamma ray distribution of nuclei is isotropic. Thus, the angular correlation between two gamma rays emitted during the cascaded gamma decay of the nucleus is due to the unequal spin states distribution in the intermediate states [1]. The main motive of the experiment is set up the experiment and investigate nuclear properties of ^{60}Co via angular correlation of $\gamma - \gamma$ cascades [1].

2 Theory

Angular correlation of gamma rays of multipole moments $L_{1,2}$ from γ-γ cascade $I_i \to I \to I_f$ is defined as

$$W(\theta) = 1 + \sum_{k=2,\text{ even}}^{k_{\max}} A_{kk} P_k(\cos\theta) \tag{1}$$

with A_{kk} (known given the information of nucleus) coefficients, $P_k(\cos\theta)$ the Legendre polynomials, and $k_{\max} = \min(2I, 2L_1, 2L_2)$[2]. Alternatively, equivalent definition is sometimes used [3]

$$W(\theta) = 1 + \sum_{1}^{l} a_i \cos^{2i}\theta \tag{2}$$

Coefficient A_{kk} is determined, generally with mixed multipole components L'_n and L_n ($n = 1, 2$), by

$$A_{kk} = A_k(L_1 L'_1 I_i I) A_k(L_2 L'_2 I_f I) \tag{3}$$

$$A_k(L_n L'_n I_{i,f} I) = \frac{F_k(L_n L_n I_{i,f} I) + 2\delta_1(\gamma) F_k(L_n L'_n I_{i,f} I) + \delta_1^2(\gamma) F_k(L'_n L'_n I_{i,f} I)}{1 + \delta_1^2(\gamma)} \tag{4}$$

$$\begin{aligned} F_k(LL'I'I) = {} & (-1)^{I'+I-1} \left[(2L+1)(2L'+1)(2I+1)(2k+1)\right]^{1/2} \\ & \times \begin{pmatrix} L & L' & k \\ 1 & -1 & 0 \end{pmatrix} \begin{Bmatrix} L & L' & k \\ I & I & I' \end{Bmatrix} \end{aligned} \tag{5}$$

$$\delta_1(\gamma) = \frac{\langle I | L'_1 \pi'_1 | I_{i,f} \rangle}{\langle I | L_1 \pi_1 | I_{i,f} \rangle} \tag{6}$$

with round brackets being $3j$-symbols and curly brackets $6j$-symbols[2]. Their value can be easily found tabulated, e.g. in [4] and [5]. $\delta_n(\gamma)$ quantifies the mixing of two multipole moments and should be determined by some other methods. If we assume $L'_n = L_n + 1$ (this is reasonable because of selection rules), then there are 7 quantum numbers to nail down the coefficients: $I_i, I, I_f, \delta_{1,2}, L_{1,2}$[2].

Example with $0 \to 1 \to 0$ γ-γ cascade. Since the first and last states are of spin 0, the multipolarities of emitted photon must be 1, thus dipole-dipole radiation. According to [3]

$$W(\theta) = 1 + \cos^2(\theta) \tag{7}$$

Plot of this angular correlation can be found in figure 1.

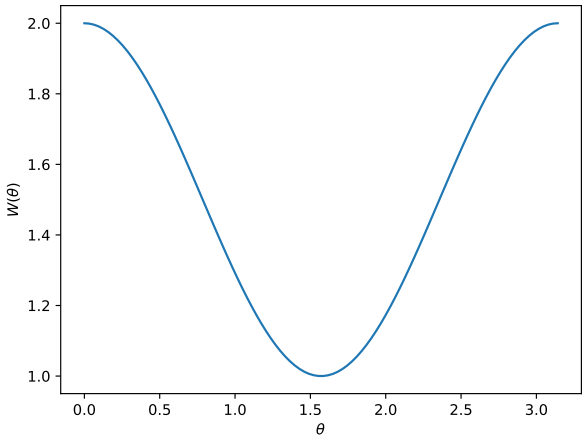

Figure 1: Angular correlation of hypothetical 010 cascade

Hyperfine structure can have influence on the angular correlation, since with quantization axis along the direction of first photon the first photon will cause transitions among the m-states. Thus in the end, the direction of second photon is altered. The perturbed angular correlation is given as

$$W(k_1, k_2, t) = \sum_{m_i, m_f, m_a, m'_a} \langle m_f | H_2 \Lambda(t) | m_a \rangle \langle m_a | H_1 | m_i \rangle \langle m_f | H_2 \Lambda(t) | m'_a \rangle^* \langle m'_a | H_1 | m_i \rangle^* \tag{8}$$

where $H_{1,2}$ represents the interaction between nucleus and radiation field and $\Lambda(t)$ is an unitary operator describing influence of extranuclear perturbation. k_1 and k_2 are wave vector of photons. [2].

Information can be obtained from measurement of γ-γ angular correlations (without extranuclear perturbation): spin angular momenta of excited states, the multipole orders, and the relative multipole composition of radiative transitions[6]. With extranuclear perturbation, we can in addition extract g-factor and quadrupole momentum of intermediate state. Internal fields of solids, liquids, and metal crystals can be investigated. And some changes in atomic shell is possible to study [2].

3 Experimental setups

3.1 Key components

Scintillation detector is used to detect ionizing radiation in general. Here we have gamma radiation. The purpose of scintillator is to lower photon energy via photoelectric effect, Compton scattering, and pair production [7]. It is then connected to photomultiplier tube (PMT) to generate signals.

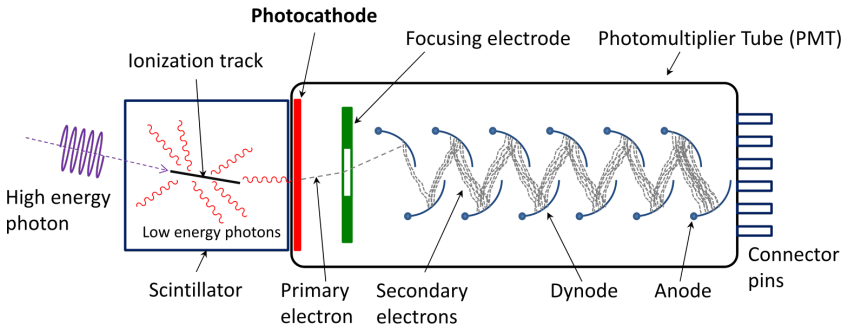

Figure 2: Scintillator with PMT [8]

Fast-slow coincidence is the technique to measure the ionizing radiation separately. The "slow" part will determine the energy of incoming radiation. And the "fast" part is used to measure the time as precisely as possible, since the photomultiplier will be brought to saturation and the height of the pulse is not proportional to radiation energy any more [9].

SCA stands for single channel analyzer. Basically it is advanced version of simple discriminator, as one can set both upper-level (ULD) and lower-level discriminator (LLD) for SCA. It reads the input pulse and check whether it is within the preset limits or not. If it is, SCA will produce a uniform digital signal. When applied to PMT, the height of pulse corresponds to energy of radiation. If SCA is built in after PMT, we are essentially picking out photons within the SCA window. Thus the name [10].

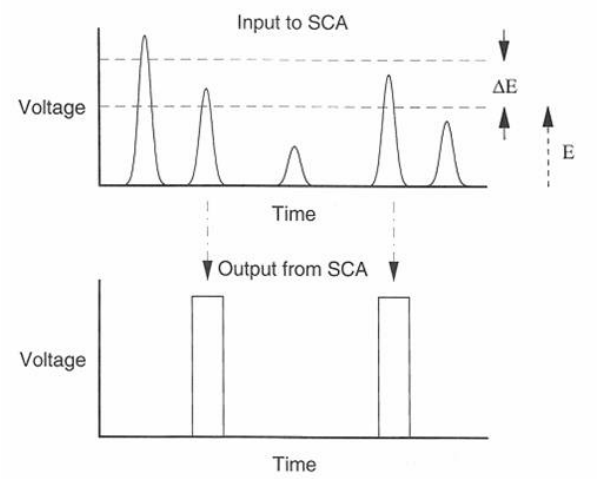

Figure 3: Single Channel Analyzer [8]

CFD stands for constant fraction discriminator. As its name suggests, it gets triggered at some preset fraction of maximal amplitude, in order to reduce "walk". In simplest form, CFD works by splitting input signals, inverting one of them, and adding delay to the other. In the end, by combining these two together, we get logic signal with minimal walk [11].

Expected Spectrum of ^{60}Co would predominantly consists of 0.31 MeV β-line and 1.1732 MeV, 1.3325 MeV γ-line [12]. Its γ-spectrum can be found in 4, where one can see two clear peaks corresponding to the γ-radiations and some background because of various effects, like pair production (higher E), Compton scattering (mid E), and photoelectric effect (low E) [7].

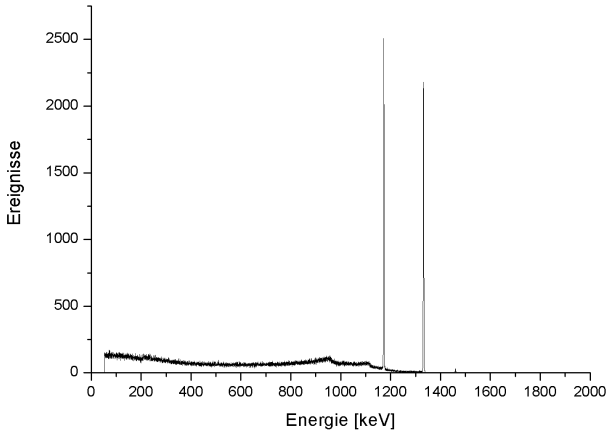

Figure 4: ^{60}Co γ-specturm [13]

4 Task for preparation

4.1 Which distances to pick?

Obviously, the count (rate) should be proportional to the solid angle ignoring the anisotropy of radiation. This assumption should not bring too much influence to the results, as long as the size of detection is accounted for in final analysis as (systematic) error. In [2], true count rate is given by

$$N_i^t(\theta) = Mp_i\Omega_i\epsilon_i \tag{9}$$

with M the number of nuclear integrations per uni time, p_i the probability that this integration is selected, Ω_i is solid angle in unit 4π, and ϵ_i the detector efficiency. According to formula of solid angle, it means that

$$N_i^t(\theta) \propto \frac{1}{r_i^2} \tag{10}$$

Follow the same principle, true number of coincidence can be written as [2]

$$C^t(\theta) = Mp_1p_2\Omega_1\epsilon_1\Omega_2\epsilon_2\epsilon_c K(\theta) \tag{11}$$

where ϵ_c is the efficiency of coincidence unit and $K(\theta)$ is the directional correlation function. $K(\theta)$ is basically the "measured" version of $W(\theta)$, i.e. what we have in the real world. The coincidence rate is then $C^t(\theta)/N_1^t(\theta)$ thus

$$\frac{C^t(\theta)}{N_1^t(\theta)} \propto \frac{1}{r_2^2} \tag{12}$$

The angular "asymmetry" is represented as the coefficients A_{kk}. With correction factor, we write

$$A_{kk} = \frac{A_{kk}^{\exp}}{Q_{kk}} \tag{13}$$

And it can be calculated by [2]

$$Q_{kk} = Q_k(1)Q_k(2) \tag{14}$$

$$Q_k(i) = \frac{J_k(i)}{J_0(i)} \tag{15}$$

$$J_k(i) = \int_0^{\pi/2} \epsilon_i(E,\alpha)P_k(\cos\alpha)\sin\alpha\,\mathrm{d}\alpha \tag{16}$$

$$\epsilon(E,\alpha) = 1 - \exp\{-\tau(E)X(\alpha)\} \tag{17}$$

with $\tau(E)$ the total absorption coefficient and $X(\alpha)$ the distance traversed in the crystal.

The correction factor will certainly affect the error of angular correlation function, multiplicatively to be specific.

According to table in [2], $h = 10\,\mathrm{cm}$ would provide the most precise measurement, since the Q_i's are closer to 1. So in the actual experiment, one can try to measure the event rate in a short time period. Then the distance should be chosen, so that enough data will be taken in the given time but still have maximal precision.

4.2 Which angles to pick?

The angular correlation function is given in the form of [1]

$$f(\theta) = A(1 + B\cos^2\theta + C\cos^4\theta) \tag{18}$$

It can be rewritten with $\alpha = B + C$ and $\beta = B - C$,

$$f(\theta) = A\left(1 + \frac{\alpha+\beta}{2}\cos^2\theta + \frac{\alpha-\beta}{2}\cos^4\theta\right) \tag{19}$$

Predicted values for A_{22} and A_{44} without mixing are given in [2]. Then the predicted correlation function is

$$\begin{aligned} W(\theta) &= 1 - \frac{A_{22}}{2} + \frac{3}{8}A_{44} + \left(\frac{3}{2}A_{22} - \frac{15}{4}A_{44}\right)\cos^2\theta + \frac{35}{8}A_{44}\cos^4\theta \\ &= 0.952412 + 0.118875\cos^2\theta + 0.039813\cos^4\theta \end{aligned} \tag{20}$$

Need to "scale" it, so that 0.9524 gets absorbed in A. Then we have

$$B = 0.124815, C = 0.041802$$

Plot correlation with these two coefficients with slight variation, we have figure. 5 From it,

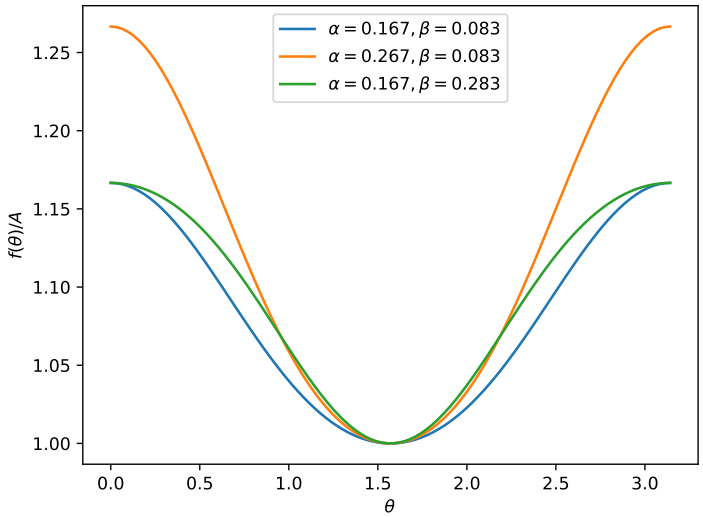

Figure 5: Correlation with different α and β

it is clear that to determine α, we need in principle only one point ($\theta = 0$ or $\theta = \pi$). But determination of β requires small increments in angle between 0 and $\pi/2$.

4.3 How to correct for de-adjustment?

In actual setup, the source might not lie perfectly in the center of circle of detectors. It will certainly cause a distortion in data, since extra "angular correlation" will be introduced. Depending on in which direction the source is off from the center of circle, the angular correlation could have an obvious asymmetry or just simply gets stretched out. To correct this, count rates of two detectors needs to be recorded. Coincidence rate should be normalized against these count rates.

5 Experimental procedure

In this experiment, we set up two detectors with equidistant from the source (5cm apart). We adjusted fast and slow signals circuits and both of them combined in to a Universal Counter(UC) through a gate and delay($G^2 - D^2$). Two CFD are connected to filter out zero crossing in fast signal circuit and two amplifiers are connected in slow signal circuit. We used three delays, two in slow signal circuit and one between CFD2 and FC. A timer connected with all counters to fixed the counting time. The figure 6 shows a schematic of the set and the tasks we did on this experiment are described in the following.

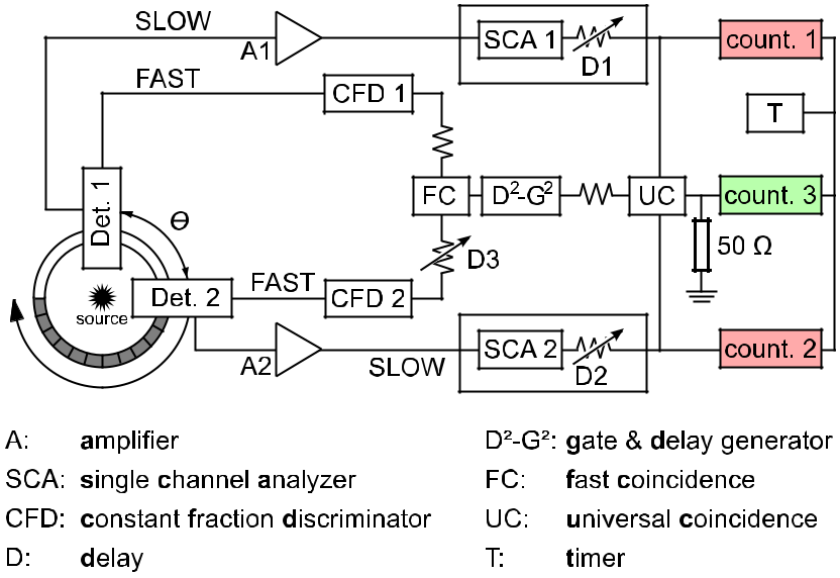

Figure 6: Set up of fast and slow coincidence circuit [1].

5.1 Adjusting the gain of the Amplifier

First, we adjusted the gain of both amplifiers (A_1 and A_2) during the set up of the experiment. The amplifiers output is linear up to $V_{max} = 9$ V. We visualized the signal, with the help of Oscilloscope, and set the amplification of amplifiers to obtain a signal with maximum around 9 V. Here we took gain of the amplifier as much as possible because larger signals are easier to process. We had been keeping in mind that the upper limit of the gain is used in the set up which is given by the signal range of the electronics. Figure 7 shows the amplified signal from the Amplifier1.

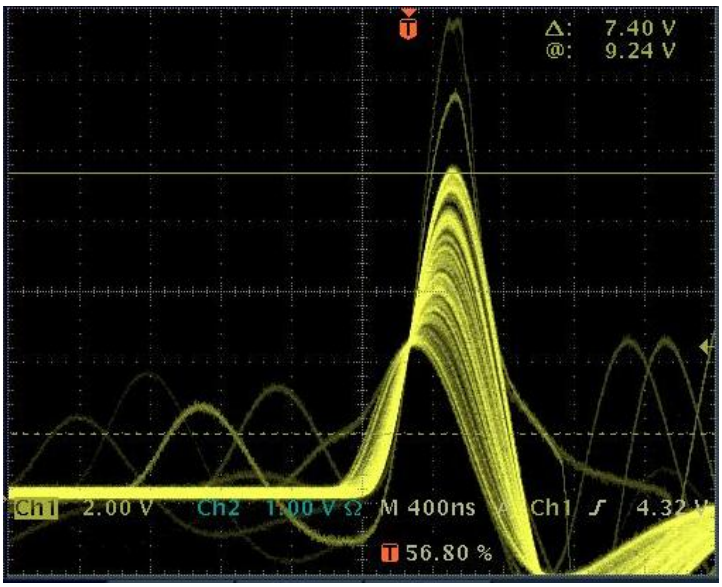

Figure 7: Amplified Signal Output from the Detector. we set the amplification of amplifiers to obtain a signal with maximum at around 9 V.

5.2 Adjusting of the CFD

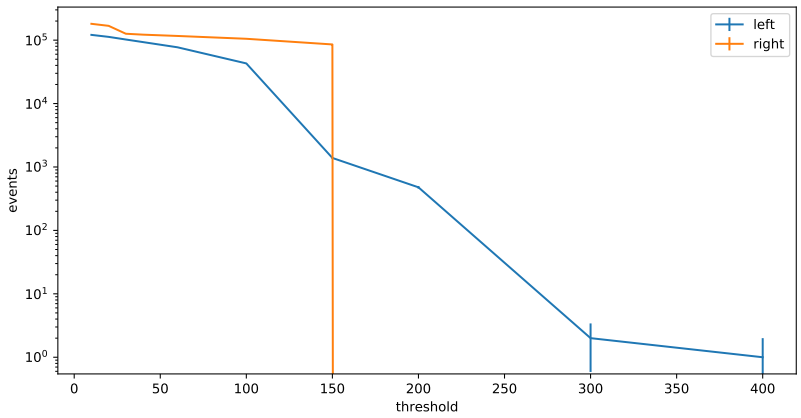

Figure 8: CFD count rate with inserting source. Here threshold limit is [150-400].

CFD has a threshold-discriminator which help to filter out zero crossing that belongs to electronic noise and not to a true scintillation signal [1]. Performing a threshold scan allows to search out the right compromise. For that, CFD has restriction upon the minimum and maximum signals and it can manage two signals of same amplitude with different risetimes. So, we have adjusted this threshold of CFD to detect only true signals not the background noise signals. In that step, We connected the negative outputs of the both CFDs to the counters and measured the count rates with and without source installed. Also, We connected a delay D_3 between CFD2 and the Fast Coincidence(FC) to correct the delay within the resolving time.

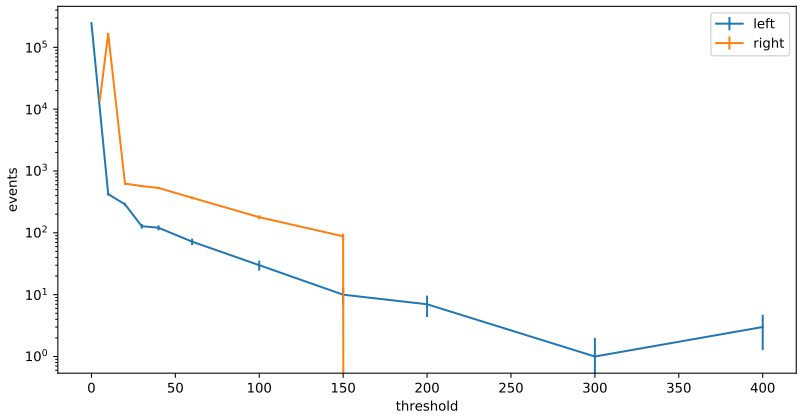

Figure 9: CFD count rate without inserting source. Here threshold limit is [150-400].

To appropriate gate duration, we calculated $\Delta N \approx \sqrt{N}$. Figure 8 and 9, respectively, shows the CDF count rate with and without inserting source.

5.3 Setting up the Fast Coincidence

Here we want to make sure that true coincidences arrive at same time (within resolving time of coincidence unit, to be precise). First, we connected both CFDs to the oscilloscope and triggered on the first channel signals. Then, on the second channel, true coincidence pulses are concentrated in small region. The random events are not the events we are looking for.

We inserted a fixed delay into one of the fast branches and a variable delay into the other one, so that we can see the full prompt curve. Then, the CFDs are connected to the fast coincidence unit and the count rates are measured for different (variable) delay with resolving time 25 ns.

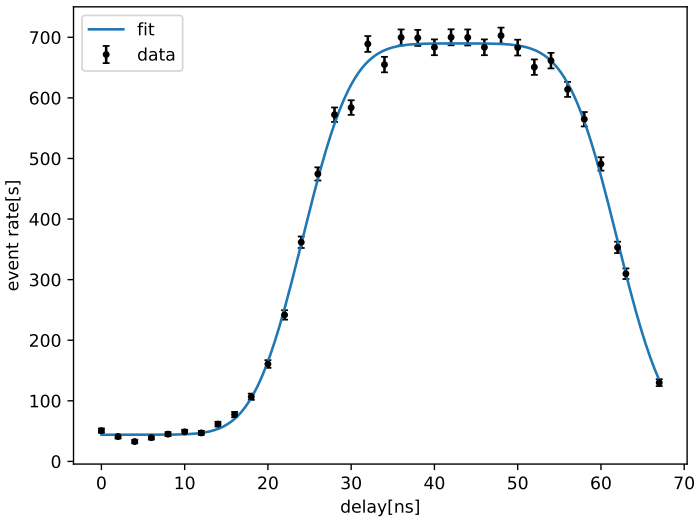

Figure 10: Prompt curve

Indeed, the prompt curve looks like a box with smeared egdges as stated in [1]. Data points are fitted wit function

$$f(t) = A_0 + A_1 \left(\frac{1}{2} + \text{erf}\left(\frac{t - t_0}{\sigma} \right) \cdot \text{erf}\left(\frac{t_1 - t}{\sigma} \right) \right) \tag{21}$$

This is reasonable considering that signals are gaussian. Data and fit curve can be found in figure 10.

These parameters each represent something physical of the experiment: A_0 random coincidence since with extreme low/high delay the true coincidences don't safisfy the conincidence criteria, A_1 related to source intensity and detector efficient, t_i resolution of corresponding detector, σ resolving time of coincidence unit. Thus the width of the plateau depends on σ. This can be easily understood as if we turn up the resolving time, then there will more events considered as coincidences. The slopes are related to detector (time) resolutions, since it smears the CFD's logic output timing. Parameter from fitting values are

$$\begin{aligned} t_0 &= 24.151 \pm 0.151 \\ t_1 &= 61.949 \pm 0.152 \\ A_0 &= 205.436 \pm 3.823 \\ A_1 &= 323.007 \pm 3.580 \\ \sigma &= 6.612 \pm 0.242 \end{aligned}$$

Correlations of parameters are quite small, since the off-diagonal entries of covariance matrix are at least one magnitude lower. Thus correlations are neglected here.

Shape of the prompt curve will change to basically flat (constant count rate) if the resolving time is chosen too short or too long, then either no signals will be picked up or every pair of inputs will be counted as coincidence.

5.4 Setting up the Slow Coincidence

Here, one hand, we connected the output from the fast coincidence unit to a gate and delay ($D^2 - G^2$) generator module to adjust the timing. Other hand, the delay of both SCAs can be adjusted. Then, the output from ($D^2 - G^2$) inserted to the first channel and positive output from SCA1 and SCA2 on after another to the second channel of the oscilloscope. We need to align the leading edges of the signal which are align the timing of these three input signals with the help of oscilloscope. Afterward, we adjusted the delays in both SCAs and ($D^2 - G^2$). In figure 11 we can see the peaks from SCAs are inside the peak of the FC unit.

5.5 Calibrating the Signal Channel Analyzer

The SCAs are used to select the whole energy deposited events of gamma rays from our source in the corresponding detector. In this step, we performed the energy calibration and recorded the energy-spectrum by using SCAs which are produces an output logic only when peak amplitude of the input signals are within threshold limit. So, For that, we set the SCAs to their window mode which is only set by second knob. Later we keep the constant obtained window size for all measured points for normalization. The window-width play important role on output. We have to marked out all structures of energy spectrum in the selective energy range, so we started with 10,...,20 window-width. we increased the window size when energy

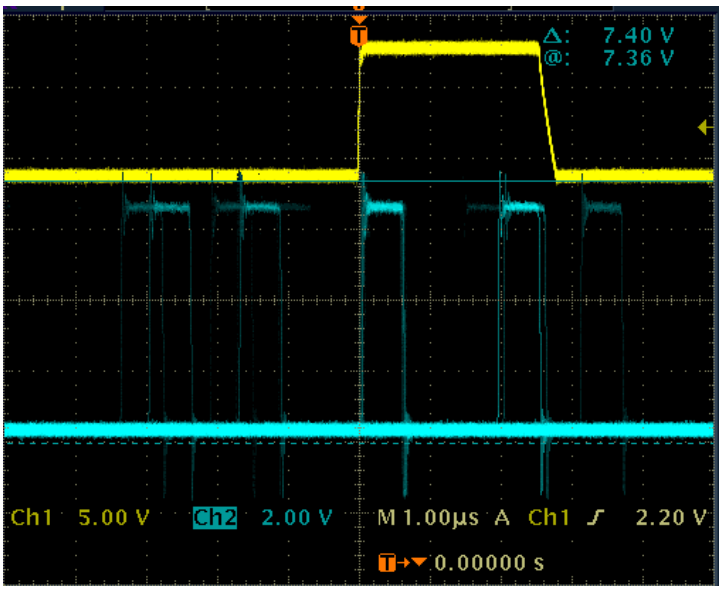

Figure 11: The timing alignment of signals from FC and two SCAs.

appeared everywhere the same count rates; however, we try to decrease the window size as much as possible. The second peak on the right counter was not appear so we changed the amplification setting. Figures 12 and 13 shows the energy spectrum of ^{60}Co-decay obtained by SCA1 and SCA2 respectively.

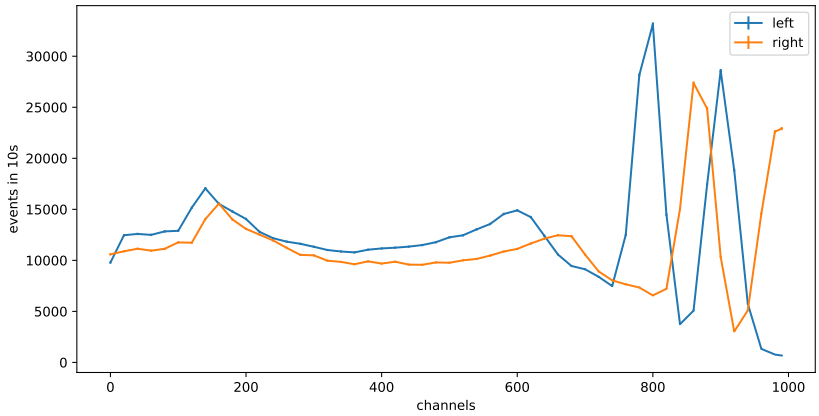

Figure 12: The energy spectra of SCA1. Here two peaks are in the range of [750-1000].

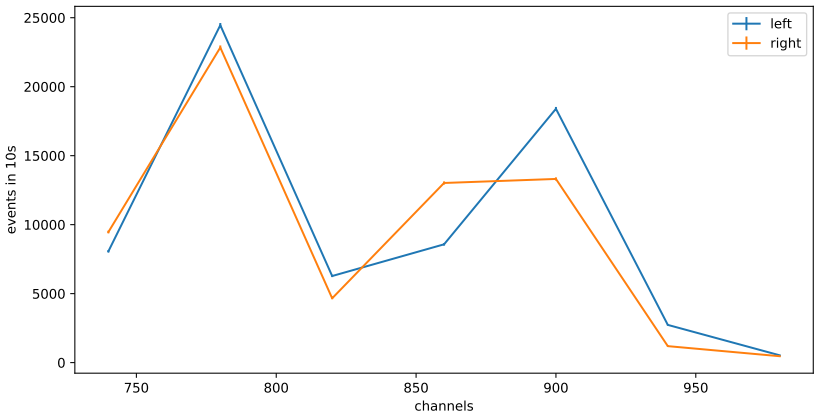

Figure 13: The energy spectra of SCA2. Here two peaks are in the range of [750-950].

5.6 Main Measurement

After adjusting all the involving apparatus in the experiment, we stated to perform the main measurement of the experiment. we used two detectors, one of them is fixed and another is movable, place at equidistant (5cm) apart from the ^{60}Co source and 180° angular separation and we adjusted the SCA windows to cover both photo peaks. Then we measured the count rates for different angles between these two detectors. We had taken more than twenty measurement with angular range of 5° some of them with 10° few were randomly. We got precise data on some positions. Specially three measurements: first one to generate the idea of the angular correlation, middle one to find out the correlation coefficient and third one to get an idea of the stability of set up. Then, we repeated the measurement on different positions.

6 Analysis

Firstly the data needs to be corrected because of random coincidences and misalignment of the setup. Random coincidence rate $\dot{R}$ is simply subtracted from the coincidence rate. In calculation of error of count rate, error of random coincidence is considered as well.

$$\dot{R} = (2.218 \pm 0.061)\,\mathrm{s}^{-1} \tag{22}$$

It is thought to be acceptable to just use one random coincidence rate for all angles, since it has no angular dependence. Effects of misalignment on random coincidence need to be considered. That is why the data get correction for misalignment after this step.

In figure. 15, one can see a clear asymmetry in count rate of the mobile detector. This can be easily explained by source not being in the center of the setup. True coincidence rate should be anti-proportional to count rates in figure. 15. Since measured angular correlation function is determined up to a proportional constant anyway, the normalization factor κ is chosen to be the fraction of count rate at smallest angle and count rate at respective angle.

Coincidence rates are normalized against the raw count rate with κ, in order to counter misalignment. True coincidence rate $\dot{C}_{\mathrm{true}}$ is calculated via

$$\dot{C}_{\mathrm{true}} = \kappa \cdot (\dot{C}_{\mathrm{measured}} - \dot{R}) \tag{23}$$

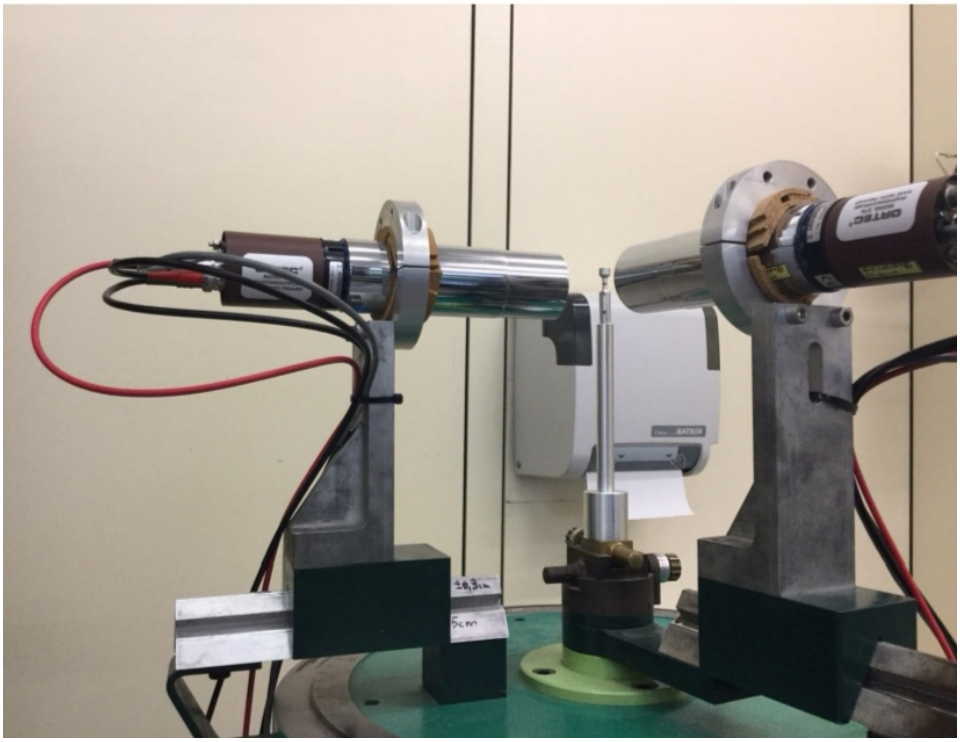

Figure 14: Set up of two detectors where one is fixed and another one is movable to rotate at a fixed radial distance from the fixed detector.

During experiment, the setup and its environment might (inevitably) change, i.e. temperature. Measurements at 180° are repeated multiple times. Some variations are seen. This introduces (one source of) systematic error and will be included in the further analysis.

$$\Delta \dot{C}_{\text{sys}} = 0.564 \tag{24}$$

Data after these corrections are plotted in figure. 16. Vertical error bars include statistical error and systematic error. Error of angle is estimated to be about 2 degrees.

	fit	theory
A	45.0721 ± 0.2578	
B	0.1246 ± 0.0310	0.1213
C	-0.0008 ± 0.0289	0.0330

Table 1: Parameters of the curve shown in figure 16 and their theoretical values after being "corrected" for finite size of detector

A least squares fit of data using function in the form of (18) is carried out. Fitted function is drawn in blue in figure 16. Parameters are shown in table 4. One should emphasize that the errors in table 4 are only the diagonal entries of covariance matrix. There are still non-vanishing off-diagonal entries, i.e. variables are somehow correlated. This is the reason why drawing confidence intervals in figure 16 is not meaningful. Covariance matrix of these fitting

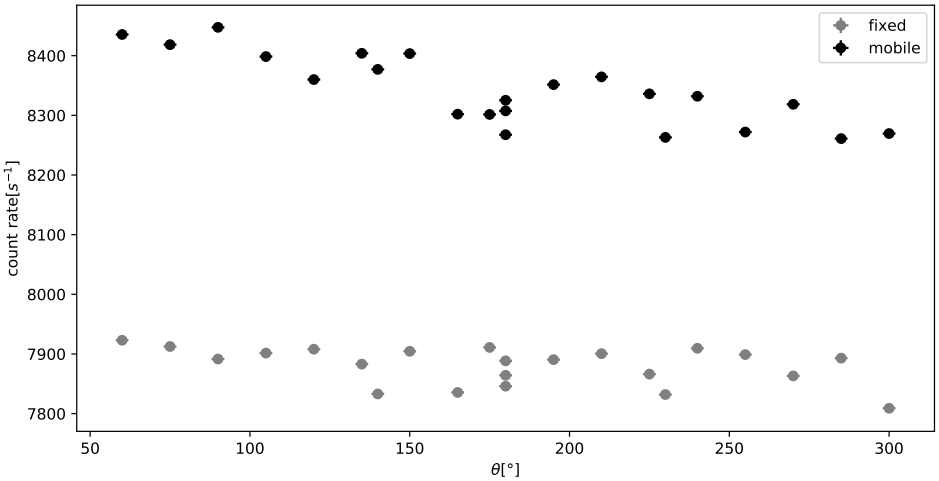

Figure 15: Raw count rate

parameters is

$$\Sigma_{ABC} = \begin{pmatrix} 0.066\,486\,01 & -0.006\,102\,61 & 0.004\,625\,04 \\ -0.006\,102\,61 & 0.000\,960\,16 & -0.000\,864\,38 \\ 0.004\,625\,04 & -0.000\,864\,38 & 0.000\,832\,77 \end{pmatrix} \tag{25}$$

Based on this value of A, we can plot the predicted function equation (20). Because of finite size of detector, prediction curve needs to be "corrected" by factor Q_k to correspond measured correlation curve. It is more convenient to apply this correction to fit curve than data points. Values of Q_k are taken from [2] with distance to source $h = 5\,\text{cm}$. Energy of γ-radiation in experiment is between 1 MeV and 1.5 MeV and only photopeaks are relevant. For convenience, mean values of Q_k of these two energies are used in calculation

$$Q_2 = 0.934,\ Q_4 = 0.792$$

Theoretical prediction with Q correction of fit parameters are also added in table 4.

It seems that prediction and measurement have at least OK agreement, only some deviation around 180° is present. But a closer look is necessary, since the fit parameters are correlated. For simplicity, we say that A has no correlation to other parameters and only its best-fit value is used. This will underestimate "distance" between theory and measurement. Taking only B and C components of equation (25), one can draw confidence intervals on parameter plane. In figure 17, one can see prediction value lie roughly 4σ away from best-fit value, even though table 4 gives us roughly 1σ accuracy.

Just as a consistency check and to better understand origin of deviation, B and C can be converted into α, β like before.

$$\begin{pmatrix} \alpha \\ \beta \end{pmatrix} = \begin{pmatrix} 1 & 1 \\ 1 & -1 \end{pmatrix} \begin{pmatrix} B \\ C \end{pmatrix} \tag{26}$$

Results are in table 2. Their covariance matrix is

$$\Sigma_{\alpha\beta} = \begin{pmatrix} 6.416\,647\,49 \times 10^{-5} & 1.273\,956\,76 \times 10^{-4} \\ 1.273\,956\,76 \times 10^{-4} & 3.521\,699\,20 \times 10^{-3} \end{pmatrix}$$

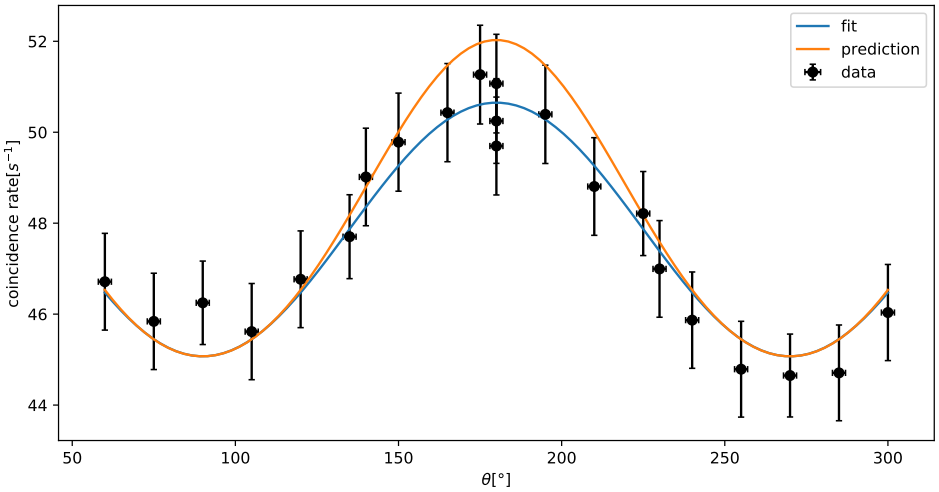

Figure 16: Angular correlation with fit and prediction

	fit	theory
α	0.1238	0.1544
β	0.1254	0.0883

Table 2: Prediction and measurement of α, β. Here theoretical value has been corrected by Q-factor.

Thus deviations are present at all angles, not e.g. only around 180° when only α is off.

There is quite obvious asymmetry (with respect to 180°) present in the angular correlation. Ideally, this should not be in data, or at least after being corrected by considering misalignment. To better see the difference, data points are plotted in figure. 18. From this, we can see that the asymmetry can be well explained by the errors.

They need to be converted to A_{kk} coefficients and then corrected for finite size of detectors. As written in equation (20), both A_{22} and A_{44} decides the values of B and C (need to scale it, so that the constant term is unity!). Thus it involves finding the inverse of the matrix. The errors here are given without correlation considered, i.e. these are only diagonal entries of covariance matrix.

	fit with correction	theory
A_{22}	0.0849 ± 0.0057	0.1020
A_{44}	-0.0002 ± 0.0063	0.0091

Table 3: Measured coefficients after corrected for finite size of detectors and theoretical values

Fitting of angular correlation could also help us to exclude other cascades. From previous found values of B and C, one can conclude that 020, 121, 220, and 320 cascades are pretty much 100% excluded using coefficients provided by [3]. Alternatively, fit function can also only contain $\cos^2\theta$ term. This fit curve visually doesn't differ from the previous curve visually, as

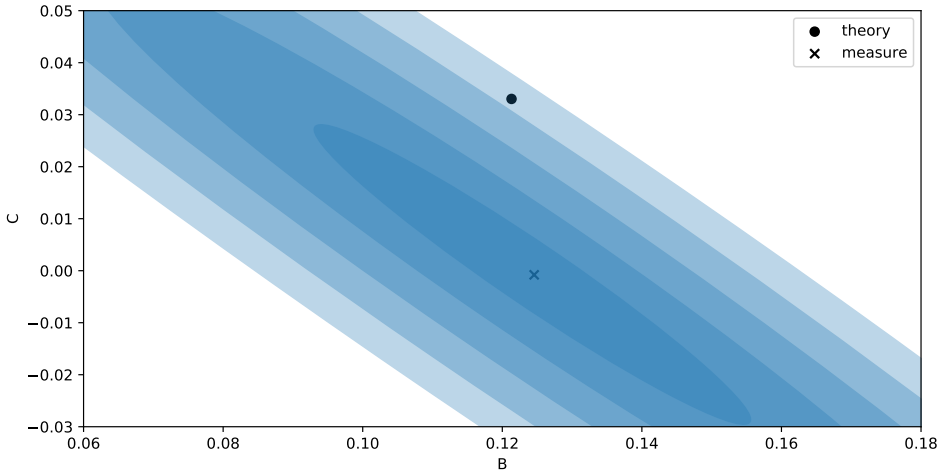

Figure 17: Regions on the plane (B, C) measured by experiment. Best-fit and theoretical prediction are included. The contours corresponds to 1σ, 2σ, 3σ, 4σ, 5σ confidence intervals.

expected since C from previous fit is almost vanishing. New fit parameters are Comparing this

	fit
A	45.0765 ± 0.1969
B	0.1237 ± 0.0077

Table 4: Parameters using alternative fit function. Errors are just the diagonal entries of covariance matrix.

B to values give in [3], the closest (positive) value is of 210 and 220 cascades with $B = 3/7 \approx 0.43$. Although Q correction is not included, we know for sure $Q \sim 1$, and measured value is no way near 0.43 (more than dozens of σs away). Some negative values are numerically closer to measured value. But from the plot, coefficient B is obviously positive. We can say for sure, measured angular correlation does not correspond to any other cascade listed in [3].

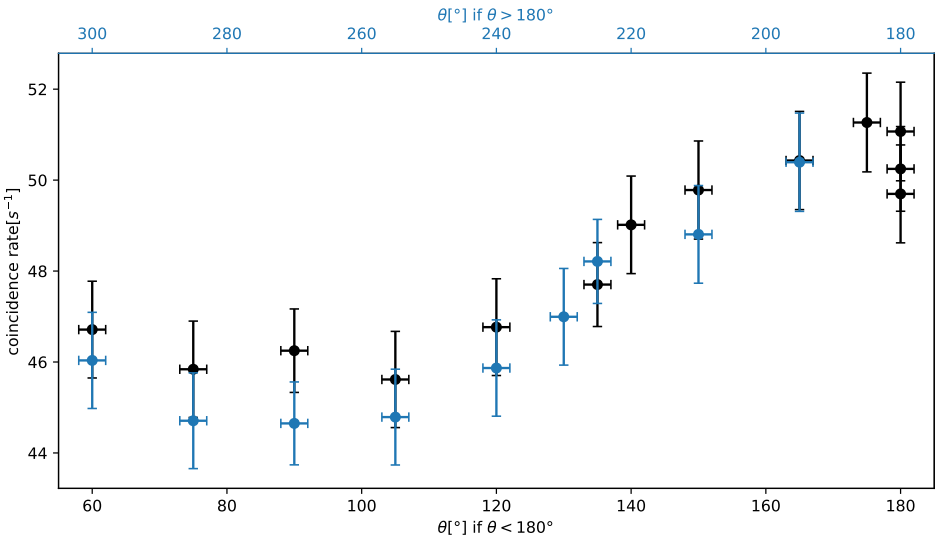

Figure 18: Angular correlation to see asymmetry. Color of data points correspond to the color of axis to use.

7 Discussion And Conclusion

In our experiment, we investigate nuclear properties of cobalt nuclei via angular correlation. After setting up all the apparatus, we measured the coincidence using two detectors one of them is fixed and another one is movable with varying angle between them. Then, we fitted the measured data with the theoretical prediction function and calculated the angular correlation coefficients: $A_{22} = 0.0849 \pm 0.0057$ and $A_{44} = -0.0002 \pm 0.0063$. The non zero values of these two angular correlation coefficients, importantly, provide strong evidence for an angular correlation between two gamma rays emitted in 010 cascade of ^{60}Co. Further investigation reveals that measured values differ from prediction by 4σ due to systematic error in the set up. On the basis of found values of B and C, we can concluded that, Other types of cascade (020,121, 220, and 320) are excluded almost 100%.

8 Acknowledgement

We would heartly acknowledge to the Bonn-Cologne Graduate School of Physics and Astronomy (BCGS) for the opportunity to perform the experiment. We would like to express our gratitude and appreciation for Dr. Christian Honisch for the tutoring, encouragement, and guidance throughout the experiment.

References

[1] Unknown. *Experiment description: Nuclear γ-γ Angular Correlations*. 2019.

[2] Kai Siegbahn, ed. *α-, β-, and γ-Ray Spectroscopy*. Vol. 2. North-Holland Publishing Company, 1965.

[3] E. L. Brady and M. Deutsch. "Angular Correlation of Successive Gamma-Rays". In: *Physical Review* 78.5 (June 1950), pp. 558–566. DOI: 10.1103/PhysRev.78.558.

[4] P.D. Stevenson. "Analytic angular momentum coupling coefficient calculators". In: *Computer Physics Communications* 147.3 (2002), pp. 853–858. ISSN: 0010-4655. DOI: https://doi.org/10.1016/S0010-4655(02)00462-9. URL: http://www.sciencedirect.com/science/article/pii/S0010465502004629.

[5] Plasma Laboratory of Weizmann Institute of Science. *369j-symbol Calculator*. URL: https://plasma-gate.weizmann.ac.il/369j.html.

[6] Robert Allan Wilson. "Directional correlation of the 346-136 keV gamma-gamma cascade in Ta181". MA thesis. Portland State University. Department of Physics, 1969. URL: https://pdxscholar.library.pdx.edu/open_access_etds/75/.

[7] Hermann Kolanoski and Norbert Wermes. *Teilchendetektoren*. Springer Berlin Heidelberg, 2016.

[8] Qwerty123uiop. *File:PhotoMultiplierTubeAndScintillator.svg*. 2013. URL: https://commons.wikimedia.org/wiki/File:PhotoMultiplierTubeAndScintillator.svg.

[9] G. Iaci and M. Lo Savio. "A fast-slow coincidence system". In: *Nuclear Instruments and Methods* 65.1 (1968), pp. 103–109. ISSN: 0029-554X. DOI: https://doi.org/10.1016/0029-554X(68)90014-1. URL: http://www.sciencedirect.com/science/article/pii/0029554X68900141.

[10] Ortec. *Single-Channel Pulse-Height Analyzers*.

[11] Canberra Elektronik. *Constant Fraction Discriminator: Model 1326, 1428* Operating Manual*.

[12] R.B.firestone. *Table of Isotopes*. 8th ed. Wiley, New York, 1996.

[13] Traitor. *File:60Co gamma spectrum energy.png*. 2007. URL: https://en.wikipedia.org/wiki/File:60Co_gamma_spectrum_energy.png.